Frequency Domain Analysis of Fuzzy B-Spline for 3D Tsunami Visualization from Remote Sensing Data

Maged Marghany[†] **and Mazlan hashim**[††]

Natural Tropical Resources Information & Mapping Research Group
(NATRIM Research Group)
Faculty of Geoinformation Science and Engineering
Universiti Teknologi Malaysia
81310 UTM, Skudai, Johore Bahru, Malaysia

Summary
This paper utilizes fuzzy B-spline based on frequency domain analysis to visualize 3D tsunami waves from remote sensing satellite data. In doing so, two dimensional Fourier transform (2DFFT) was used to extract the successive tsunami wave characteristics i.e. frequency, wavelength, direction and energy. In this context, fuzzy B-spline was utilized to reconstruct a global topographic structure between the data points, were used to support an approximation to the real successive tsunami wave propagation

Keywords**:** Frequency domain, 2DFFT, fuzzy B-spline, 3D visualization, Tsunami wave.

1. Introduction

The most principle techniques for three dimensional image display are involving the stereoscopic display, the volume scanning type display, the lenticular type display, and the holographic video display. Therefore, these are required the large form of three-dimensional scalar and vector field samples. Nevertheless, 3-D image visualization or display requires huge amount of data to acquire the stereoscopic visual demands [8 & 4]. However, the stereoscopic visual can have a dramatic impact on the 3-D image display which can be appears as artifact effect [5]. In this context, Mihajlovic et al.,[12] introduced a frequency domain analysis of B-spline and classified the parameter space into different regions of dominant reconstruction artifacts. In order to analyze, classify and estimate the error of the applied filters, they have used Taylor Series expansion of the convolution sum. Therefore, Anile [1] introduced direct and indirect spline transform to achieve efficient scaling mechanisms and re-sampling of the data volume and interpolation.

At present, there are few studies have quantified the damages and rate changes along coastal regions [4, 5, 10].Yet, the dynamic of successive tsunami wave characteristics has not been accounted. Salinas et al., [13] have studied the fundamental properties of the tsunami wave propagations from SPOT-4 imagery which was acquired 20 minutes after the first wave arrival to the port of Phuket, Thailand. They have used two scan lines were layered over the selected wave pattern and plotted as a function of distance to retrieve the tsunami wavelength. Nevertheless, scientists and researchers have agreed that prior to map wave spectra were extracted from satellite data, 2 DFFT must be used to convert the satellite data into frequency domain [16 & 10]. In this context, both linear and nonlinear algorithms have used to retrieve wave characteristics from satellite imagery. In addition, for SPOT-4, there are several parameters could be influenced the image qualities: (i) angular dispersion, wavelength, and wave height, (ii) weather conditions which involves cloud cover and visibility and (iii) the sum of the sun elevation angle and the viewing incidence [15].

Salinas et al., [13] have attempted to model the run-up from SPOT-5 by involving beach slope and physical wave spectra properties from SPOT-5 imagery which were retrieved by method of Salinas et al., [13]. In fact, the tsunami wave properties such as frequency, wavelength, and wave height are required to be fit in run-up model. Moreover, the beach slope surveying after the event must not be taken into account due to the rapid dynamic changes of coastal geomorphology in short period due to the quick change in coastal water dynamic movements. In addition, run-up model is required too accurate DEMs of coastal zones. However, Salinas et al., [13] stated that to approach the run–up and inundation problem, the non–linear shallow water equations must be solved with an appropriate treatment for breaking waves and moving shore lines. Moreover, they have reported that the complex geometry of the coastal line coupled with arbitrary beach and sea floor profiles, makes solving the shallow water equations a formidable task which can only be approached numerically.

Manuscript received May 5, 2009
Manuscript revised May 20, 2009

In this context, the standard methods are required to acquire accurate successive tsunami wave propagations from satellite imagery and to avoid uncertainty might be arisen due to absence of real time in situ measurements. In modeling dynamic pattern from the satellite imagery, image processing uncertainty is major challenges.

In this paper, we address the question of 3-D tsunami wave propagation and run-up reconstructions using Quickbird imagery without needing any in situ wave measurements. This is demonstrated with using fuzzy B-spline. Three hypothesis examined are: (i) the main algorithm of fuzzy B-spline is modified based on frequency domain analysis; (ii) reconstruction of 3D tsunami propagation from satellite Quickbird imagery is required to reconstruct impulse function from the known tsunami spectra is derived by 2-DFFT, (iii) 3rd order B-spline interpolation can be used to invert 2D tsunami spectra into 3-D successive tsunami propagation and run-up.

2. Model

2.1 Wave Spectra Estimation from QUICKBIRD Satellite Data

The basic concept is to capture an image of the instantaneous wave propagation along the coastal water, assuming that grey level variation of the image contain the wave information. In fact, the optical sensor is captured the amount of the radiance have reflected from the objects. The radiance that is received at the sensor is dominated by the background sky radiance that is reflected from the ocean surface [10]. This radiance field is modulated spatially and temporally by the slopes of the waves as they propagate. Wave visibility is enhanced in sunny conditions looking close to the specular reflection direction. When the sea surface is modulated by sinusoidal movement, the specular vector is no longer unidirectional, but varies with the wave slope symmemetrically which remain small as wave slopes reach few degrees. Specular reflection is function of the sun elevation angle and the viewing incidence with respect to the vertical. Populus et al.,[15] reported that the sum value of viewing incidence and sun elevation must be above 60 ^{o}for wave to be clearly visible in SPOT data. Another factor seems to influence the optical image quality is: angular dispersion, wavelength and wave height. Since the wave changes its direction and wavelength as it propagates, the two dimensional Discrete Fourier Transform (2DFFT) was used to derive the wave number spectra from Quickbird data. First, choose a window kernel size of 512 x 512 with the pixel size equal to ΔX . Following Maged [9] and Maged and Mazlan [11], let $X(m_1, m_2)$ represent the digital count of the pixel at (m_1, m_2) which is used to perform 2 DFFT, which is given as

$$F(kx, ky) = N^{-2} \sum_{m_2=0}^{N-1} \left[\sum_{m_1=0}^{N-1} X(m_1, m_2).e^{-ikx.m_1.\Delta X} \right] .e^{-iky.m_2.\Delta X} \quad (1)$$

where, $n_1 and n_2 = 1,2,3,......., N$ and kx and ky are the wave numbers in the x and y directions, respectively. Following, Gota and Ogawa[6] the run-up is estimated by

$$R = \left[J_0^{\,2}(\frac{4\pi l}{L}) + J_1^{\,2}(\frac{4\pi l}{L}) \right]^{-1} 4[\iint E(k_x, k_y) dk_x dk_y]^{0.5} \quad (2)$$

where $E(k_x, k_y)$ is spectra energy, L wavelength are derived from 2 DFFT according to Populus et al.,[15], J_0, J_1 are the Bessel functions of the first kind of order 0 and 1, and l is the horizontal distance between toe of the slope and the shoreline.

2.2 Fuzzy B-spline Method

2.2.1 Frequency Domain of B-spline

The analysis of B-splines in frequency domain is required to determine the impulse response of B-spline interpolation which denotes any function in a continuous domain (or more correctly: distribution) that has a form of the Dirac's ∂ distribution wave trains with the varying discrete sequence of tsunami wave amplitudes. The basic step in the reconstruction process is the construction of the continuous function from discrete frequency sample values. In further analysis, the impulse function is created from the known samples. The B-spline weight functions are continuous functions and sampling β_n of these functions can be applied. According to Mihajlovic et al.,[12], the frequency domain analysis of B-spline F_n is given by

$$F_n = \hat{f}(\omega) \frac{\sin c^{n+1}(\frac{\omega}{2\pi})}{\beta_n(0) + 2\sum_{k=1}^{0.5n} \beta_n(k) \cos(k\omega)} \quad (3)$$

where $\beta_n(k)$ the discrete Fourier is transform of sequence samples from selected kernel windows in Quickbird imagery, $\hat{f}(\omega)$ is Fourier frequency domain which obtained from equation 1. Equation 3 is considered as correction to the B-spline, so its frequency response is wider. Increasing order n leads to frequency response which is getting closer to the ideal low-pass filter.

2.2.2 Fuzzy B-spline Method

The fuzzy B-splines (FBS) are introduced allowing fuzzy numbers instead of intervals in the definition of the frequency domain of B-spline. A fuzzy number is defined using interval analysis. There are two basic notions that we combined together: confidence interval and presumption level. A confidence interval is a real values interval which provides the sharpest enclosing range for tsunami wave spectra propagation in spatial domain. An assumption level μ -level is an estimated truth value in the [0, 1] interval on our knowledge level of the Tsunami wave spectra[1]. The 0 value corresponds to minimum knowledge of tsunami frequency spectra, and 1 to the maximum variation in tsunami frequency spectra was retrieved from Quickbird imagery. A fuzzy number is then prearranged in the confidence interval set, each one related to an assumption level $\mu \in [0, 1]$. Moreover, the following must hold for each pair of confidence intervals which define a number: $\mu \succ \mu' \Rightarrow \omega \succ \omega'$. Let us consider a function $f : \omega \rightarrow \omega'$, of N fuzzy variables $\omega_1, \omega_2, ..., \omega_n$. Where ω_n are the global minimum and maximum values of the function on the tsunami frequency spectra. Based on the spatial variation of the tsunami spectra propagation, the fuzzy B-spline algorithm is used to compute the function *f*. Following Anile et al.,[2] a fuzzy B-spline f_{BS} relative to crisp knot sequences ($\beta_1, \beta_2, ..., \beta_m$) , *m=q+2(n-1)* is function from the real curve to the set of real fuzzy numbers:

$$f_{\beta S} = \sum_{i=0}^{q+2(n-1)} f_i F_{n_{i,p}}(\beta_n) \qquad (4)$$

where f_i is the control coefficient, are fuzzy numbers and $F_{n_{i,p}}(\beta_n)$ are the crisp frequency domain of B-spline function of order of *n*.

3. Results and Discussion

Fig. 1 shows the images were acquired by the Digital Globe Quickbird satellite data. It shows a portion of the southwest coast of Sri Lanka, by the town of Kalutara (Fig. 1). The images were acquired on Sunday December 26, 2004, at 10:20 am local time, slightly less than four hours after the 6:28 a.m. (local Sri Lanka time) earthquake and shortly after the moment of tsunami impact. The tsunami first impacted the eastern coastline of Sri Lanka shortly after 8:00 am and then swept along the southern and south-western shores over the following 90 min or so. Its effects were inconsistent from place to place, but in general the eastern, north-eastern and south eastern coastline was particularly hard hit, while the waves refracted around the island to devastate the southern and south-western coast in a patchy manner.

(a) (b)

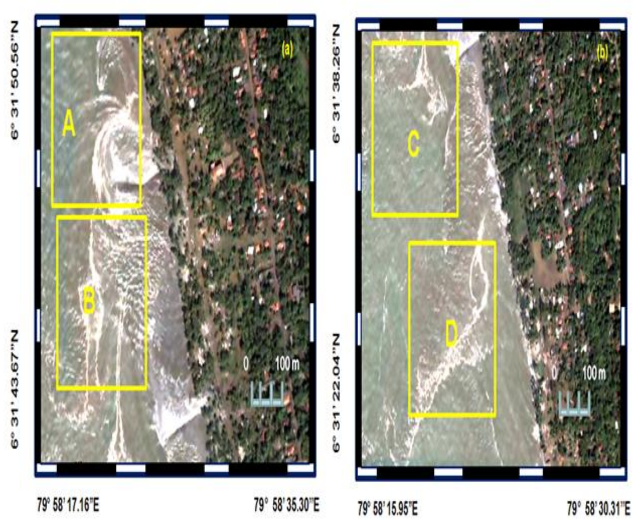

Fig. 1. Quickbird imagery in (a) North of Kalutra and (b) South of Kalutra

Fig.2 shows the spatial frequencies of tsunami spectra have extracted through 2 DFFT. The lower frequencies in the scene are plotted at the center of the spectrum and progressively higher frequencies are plotted outward. In this approach, the spectra wavelengths are proportional inversely with the frequencies. In this context, the tsunami spectra are illustrated in polar plots (Fig.2). The circular areas indicate the individual wavelength peak spectra propagation. The scale indicates the change of wavelength spectra in the circular areas with distance of the peaks from the center being inversely proportional towards its wavelength. The angular position of the peaks indicates the wave propagation direction, which are inherently ambiguities with the 180°, which has also been found by Maged [9].

Figs. 2a and 2b show different pattern of tsunami wave spectra along the Sri Lanka coastal waters. Fig. 2a depicts tsunami wave spectra direction of 150° towards the coastline while Fig. 2b shows wave propagation towards 70°. It is interesting to find that the dominant wave lengths were between 50 and 140 m. The change of direction pattern from window A to window B which was due to diffraction impact. This could be contributed to that tsunami waves have diffracted around Sri-Lanka Island and then moved perpendicular to the Kalutara coast and spread inland, causing widespread flooding. Fig. 1a shows that the water drained back into the ocean it built two barriers along Kalutara coastline. As successive tsunami passed the large barrier, the tsunami wave spread along the crest behind the barrier. It was diffracted so that the barrier stopped part of the wave crest and rest it passed by to generate a large eddy with the radius of 150 m behind the barrier. This indicates that the successive tsunami waves hit the Kalutara coastline have induces changes of the coastal zone morphology features [11]. A few minutes later, new series of tsunami wave spectra struck the coastline with wavelength ranged between 50-100 m and dominant direction of 60 °towards the shoreline (Figs. 2c and 2d).

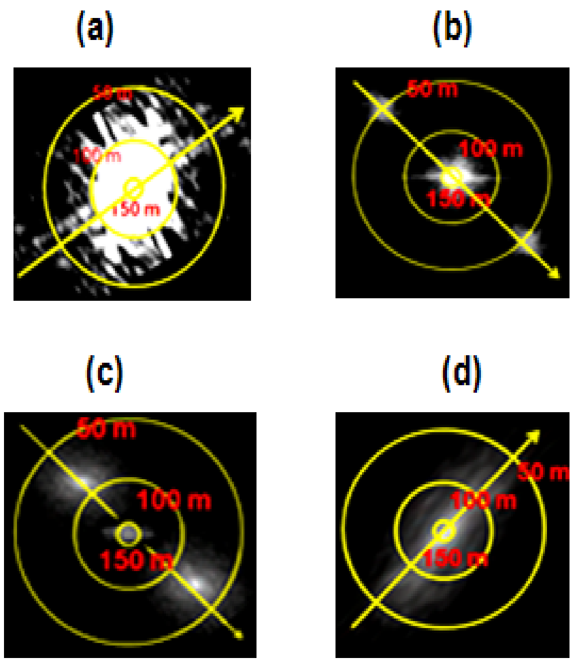

Fig. 2. Tsunami wave spectra were derived from Fig. 1 at (a) window A,(b), window B, (c) window C, and (d) window D.

Fig. 3 shows the wave spectra energy estimated in areas A and B. The spectra density of the wave diffraction due to the barriers is 10 m^2 /Hz within narrow wave number spectra band of 0.13 rad/m. This indicates highest amount of spectra energy have input along the coastline of Kalutara due to the wave diffraction around Sri- Lanka.

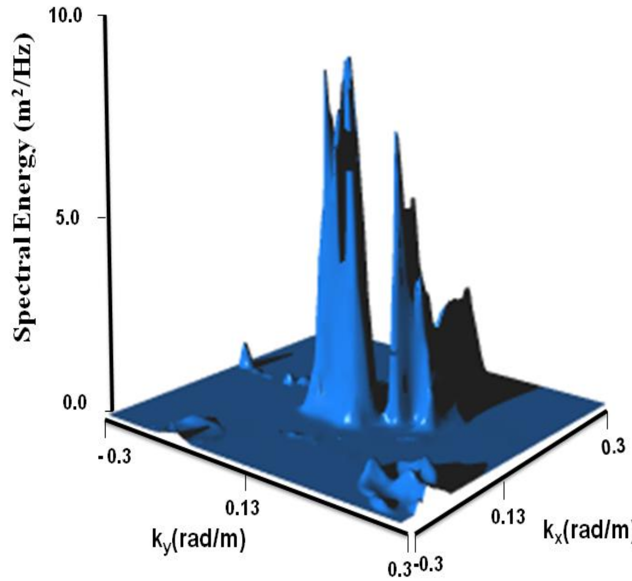

Fig. 3. Wave spectra energy in windows A and B

Fig. 4 shows the 3D tsunami wave propagations constructed by using fuzzy B-spline. It is interested to find the clear structure of tsunami wave heights which are between 3 and 6 m. The maximum wave height of 6 m was due to the wave breaking. The maximum wave height is shown across an eddy movement while the waves have spread inland was between 4 and 6 m height. Fig. 2a shows 3-D dimensions for wave diffraction along Kalutara coastline. This indicates that turbulent water movement due to combination of wave diffraction, refraction, reflection and longshore current movements between the two barriers. Taken together, these were able to cause a pattern which spell out, approximately the pattern of the Arabic word for Allah as shown in Fig. 1a and El-Gbar as shown in Fig. 1b.

Figs. 4a and 4b show that the run-up ranged between 4 and 6 m. The minimum run-up observed inland while the regions were closed to the coastline dominated by run-up of 6 m (Fig. 4). It is obvious that the mechanism of run-up was accompanied by convergence zone (Fig. 4).

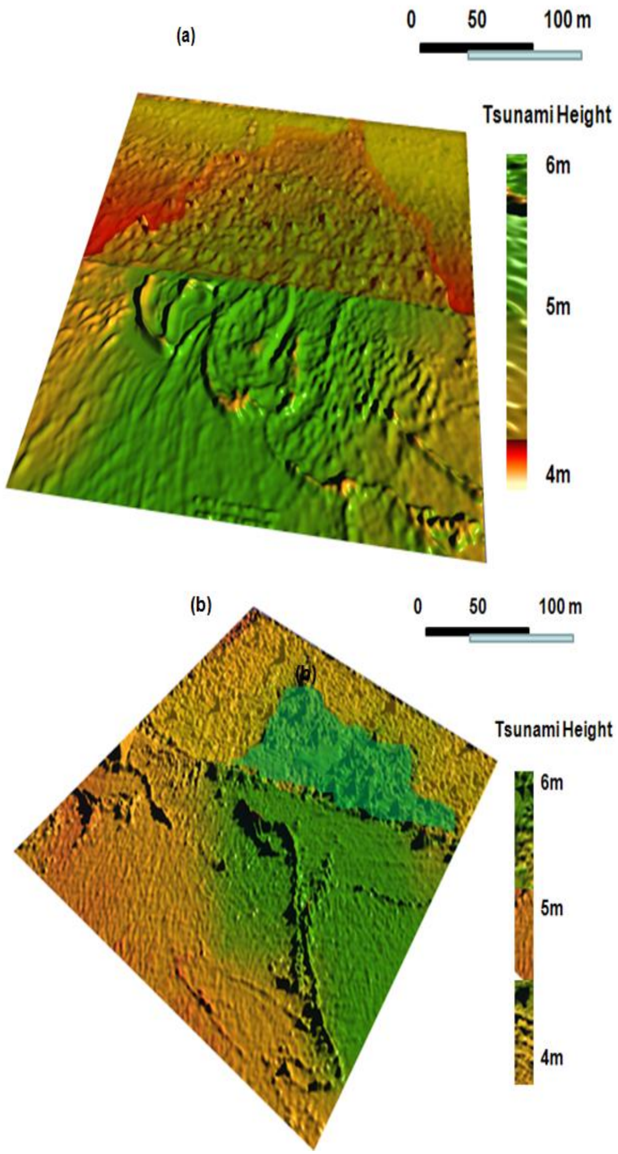

Fig. 4. Fuzzy B-spline 3D tsunami wave propagations and run-up in (a) north and (b) south of Kalutara coastline.

Fuzzy B-spline approximation of 3^{rd} order provides 3D images which were virtually free of visible artifacts. This is contributed due to the fact that each operation on a fuzzy number becomes a sequence of corresponding operations on the respective μ-levels , and the multiple occurrences of the same fuzzy parameters evaluated as a result of the function on fuzzy variables [1&2]. It is very easy to distinguish between small and long waves. Typically, in computer graphics, two objective quality definitions for fuzzy B-spline were used: triangle-based criteria and edge-based criteria. Triangle-based criteria follow the rule of maximization or minimization, respectively, of the angles of each triangle[7]. The so-called max-min angle criterion prefers short triangles with obtuse angles. This finding confirms those of Keppel [8] and Anile [1].

4. Conclusions

This work has demonstarted the possibilities of three-dimensional tsunami wave reconstruction using fuzzy B-spline from high resoltution QuickBird satellite data. The basic step in the reconstruction process was the construction of the continuous function from discrete sample values of frequency spectra which are acquired using 2DFFT. This study shows different pattern of tsunami wave spectra along the coastal water of Sri Lanka. In northern part of Kalutara, tsunami wave spectra have direction of 150° towards the coastline while in southern part, tsunami wave spectra have direction of 70°. It is interesting to find that the dominant wave length was between 50 and 140 m. The change of direction pattern was due to diffraction and reflection impact. Further, the maximum spectra energy was is 10 m^2 /Hz within narrow wave number spectra band of 0.13 rad/m. Finally, tsunami wave run-up was between 4 and 6 m height. In conclusion, the involving of frequency response analysis with fuzzy B-spline can be used as method for 3D reconstruction of coastal wave propagations from high resolution satellite data.

References

[1] Anile, A. M, (1997) *Report on the activity of the fuzzy soft computing group*, Technical Report of the Dept. of Mathematics, University of Catania, March 1997, 10 pages.

[2] Anile, AM, Deodato, S, Privitera, G, (1995) *Implementing fuzzy arithmetic*, Fuzzy Sets and Systems, 72,123-156.

[3] Anile, A.M., Gallo, G., Perfilieva, I., (1997) *Determination of Membership Function for Cluster of Geographical data*. Genova, Italy: Institute for Applied Mathematics, National Research Council, University of Catania, Italy, October 1997, 25p. Technical Report No.26/97.

[4] Chen, P., Liew, S., Liew C., and Kwoh. L. K., (2005), Tsunami damage assessment using high resolution satellite imagery: A case study of Aceh, Indonesia, *Proc. IEEE International Geosciences and Remote Sensing Symposium 2005*, 25 - 29 July 2005, Seoul, Korea.

[5] Chia, A. S., Liew,S. C., Heng, A. W. C.,and Kwoh L. K. (2005), Satellite observations of coastline changes in the Andaman islands after the 2004 Sumatra earthquake, *Proc. IEEE International Geoscience and Remote Sensing Symposium 2005*, 25 - 29 July 2005, Seoul, Korea.

[6] Goto, C. and Y. Ogawa, (1992). Numerical Method of Tsunami Simulation with the Leap-frog Scheme. Dept. of Civil Engineering, Tohoku University. Translated for the TIME Project by N. Shuto.

[7] Fuchs, H. Z.M. Kedem, and S.P.Uselton. (1977) Optimal Surface Reconstruction from Planar Contours. *Communications of the ACM*, **20**, 693-702.

[8] Keppel, E. (1975) Approximation Complex Surfaces by Triangulations of Contour Lines. *IBM Journal of Research Development*, **19**, 2-11
[9] Maged, M.M, (2001). Operational of Canny algorithm on SAR data for modeling shoreline change. Photogrammetrie Fernerkundung Geoinformation 2, 93-102.
[10] Maged, M.M and M.Sufian (2005) "Simulation of The Successive Tsunami Waves along Kalatura Coastline from Quickbird-1 satellite", Asian Journal of Geoinformatics, Vol. 5, No.2, May 2005.
[11] Maged, M., and M., Hashim (2007). Fuzzy B-spline For 3D Tsunami Wave Reconstruction from Quickbird Data. CD-Proceedings of The 28 th Asian Conference on Remote Sensing, 12-16 November 2007, Putra World Trade Center (PWTC) Kuala Lumpur, Malaysia.http://www.aarsacrs.org/acrs/proceeding/ACRS2007/Papers/Ps1.G5.9.pdf, pp:1-6.
[12] Mihajlovic, Z. Goluban, A. and Zagar, M (1999). Frequency Domain Analysis of B-spline Interpolation, July 12-16 1999, Bled Slovenia, Vol. 1. pp: 193-198.
[13] Salinas, S. V., Low J. K. K., and Liew, S. C., (2005), Quick analysis of wave patterns generated by tsunami waves and captured by SPOT imagery, *Proc. IEEE International Geosciences and Remote Sensing Symposium 2005*, 25 - 29 July 2005, Seoul, Korea.
[14] Salinas, S. V., Cortijo, P. Chen, and Liew S. C., (2006), Tsunami Effects on Shallow Waters : From Wave Scattering to Land Inundation, *Proc. IEEE International Geosciences and Remote Sensing Symposium 2006*, 31 July - 4 August, Denver, Colorado, USA, pp. 3357 – 3360.
[15] Populus J.,Aristaghes, C., Jonsson,L., Augustin, J.M., Pouliquen, E., (1991). The use of SPOT data for wave analysis. *Journal Remote Sensing Environ*ment 36, 55-65.
[16] Vachon P.W., K.E. Harold and J. Scott. (1994). Airborne and Space-borne Synthetic Aperture Radar Observations of ocean waves. *Journal of Atmospheric.-Ocean* 32 (10); 83-112.

Dr. Maged Marghany *is a senior lecturer at* the Faculty of Geoinformation Science & Engineering,, Natural Tropical Resources Information & Mapping Research Group, *Universiti Teknologi Malaysia* (UTM). He holds B.C. Physical oceanography degree from Alexandria University, M.Sc degree from University Putra Malaysia, Malaysia and a PhD in Environmental remote sensing from University Putra Malaysia, Malaysia. He awarded ESA post-doctoral fellowship at ITC, The Netherlands. His research interests lie in the areas of radar satellite applications to coastal studies He has authored over 100 articles in both international and national refereed journals, conference proceedings, and workshop in field of microwave application to coastal studies such as ocean wave spectra, modeling shoreline change and oil spill trajectory movements.

Dr Mazlan Hashim is currently a Professor of Remote Sensing at the Faculty of Geoinformation Science & Engineering, *Universiti Teknologi Malaysia* (UTM). He holds B.Surveying degree from UTM, Master Engineering degree from University of New Brunswick, Canada and a PhD in environmental remote sensing from University of Stirling, United Kingdom. His research interests lie in the areas of satellite remote sensing mission analysis, satellite digital image processing inclusive of calibrating and validating satellite image products. He has authored/coauthored over 200 articles in both international and national refereed journals, conference proceedings, workshop and monographs in field of remote sensing, digital image processing and related technologies.